Diabetes, Metabolic Syndrome and Obesity

Dovepress
Taylor & Francis Group

Open Access Full Text Article

ORIGINAL RESEARCH

Jiangzhi Granule Ameliorates JNK-Mediated Mitochondrial Dysfunction to Reduce Lipotoxic Liver Injury in NASH

Yuwei Jiang[1,*], Jiaoya Xu[1,2,*], Junyao Ding[1,*], Tao Liu[1], Yang Liu[1,3], Ping Huang[1], Qianlei Wang[1], Peiyong Zheng[1], Haiyan Song[1], Lili Yang[1]

[1]Institute of Digestive Diseases, Longhua Hospital, Shanghai University of Traditional Chinese Medicine, Shanghai, People's Republic of China; [2]Department of Gout, Guanghua Hospital, Shanghai University of Traditional Chinese Medicine, Shanghai, People's Republic of China; [3]Teaching Experiment Center, Shanghai University of Traditional Chinese Medicine, Shanghai, People's Republic of China

*These authors contributed equally to this work

Correspondence: Haiyan Song; Lili Yang, Institute of Digestive Diseases, Longhua Hospital, Shanghai University of Traditional Chinese Medicine, 725 South Wanping Road, Shanghai, 200032, People's Republic of China, Email songhy@126.com; yanglili76@126.com

Purpose: Mitochondrial dysfunction mediated by c-Jun N-terminal kinase (JNK) plays an important role in lipotoxic liver injury in nonalcoholic steatohepatitis (NASH). This study aims to investigate the pharmacological mechanism of Jiangzhi Granule (JZG), a Chinese herbal formula against NASH, with a focus on its regulation of JNK signaling-mediated mitochondrial function.

Methods: Hepatocytes were induced by palmitic acid (PA) for 24 h to establish an in vitro lipotoxic model, which was simultaneously treated with either JZG or vehicle control. Male C57BL/6J mice were fed a high-fat diet (HFD) for 22 weeks and then treated with JZG via gavage for additional 8 weeks. Lipotoxic injury in hepatocytes or mice liver tissues, as well as JNK signaling-related molecules, were further investigated.

Results: JZG improved PA-induced lipid deposition, cell viability, apoptosis, and mitochondrial dysfunction in hepatocytes. In NASH mice, JZG reduced hepatosteatosis, and inflammatory infiltration, and improved mitochondrial morphology and quantity in liver tissues. Additionally, elevated phosphorylation ratio of non-receptor tyrosine kinase c-Src (Src) and reduced phosphorylation ratio of JNK and SH2-containing protein tyrosine phosphatase (SHP-1) were found in both hepatocytes and mice liver tissues treated with JZG versus those with the vehicle.

Conclusion: Taken together, JZG could improve mitochondrial dysfunction and reduce lipotoxic liver injury in NASH in vivo and in vitro models. The inhibition of the JNK signaling pathway may contribute to the underlying mechanism of JZG in preventing and reversing NASH development.

Keywords: nonalcoholic steatohepatitis, Jiangzhi Granule, c-Jun N-terminal kinase, mitochondrial dysfunction, lipotoxic injury

Introduction

Nonalcoholic fatty liver disease (NAFLD) is a metabolic disorder characterized by excessive lipid accumulation in the liver. The global prevalence of NAFLD has been continuously increasing, currently affecting an estimated 20–30% of adults, and over 75% of those with obesity.[1] Histologically, it is divided into nonalcoholic fatty liver (NAFL) and nonalcoholic steatohepatitis (NASH). The latter represents a more advanced stage, characterized by inflammation, hepatocyte ballooning, and the potential for fibrosis development, in addition to lipid deposition in liver tissues. NASH has recently emerged as a major cause of end-stage liver dysfunction.[2] Evidence indicates that approximately 10–25% of NASH patients may progress to cirrhosis,[3] and it is predicted that NASH-related cirrhosis would become the leading cause of liver transplant in the next decade.[4]

The "multiple hit" hypothesis is recognized as the predominant explanation for the pathogenesis of NAFLD. It assumes that the excessive accumulation of free fatty acids (FAs) triggers a series of deleterious events, including

Received: 10 September 2024
Accepted: 28 December 2024
Published: 6 January 2025

Graphical Abstract

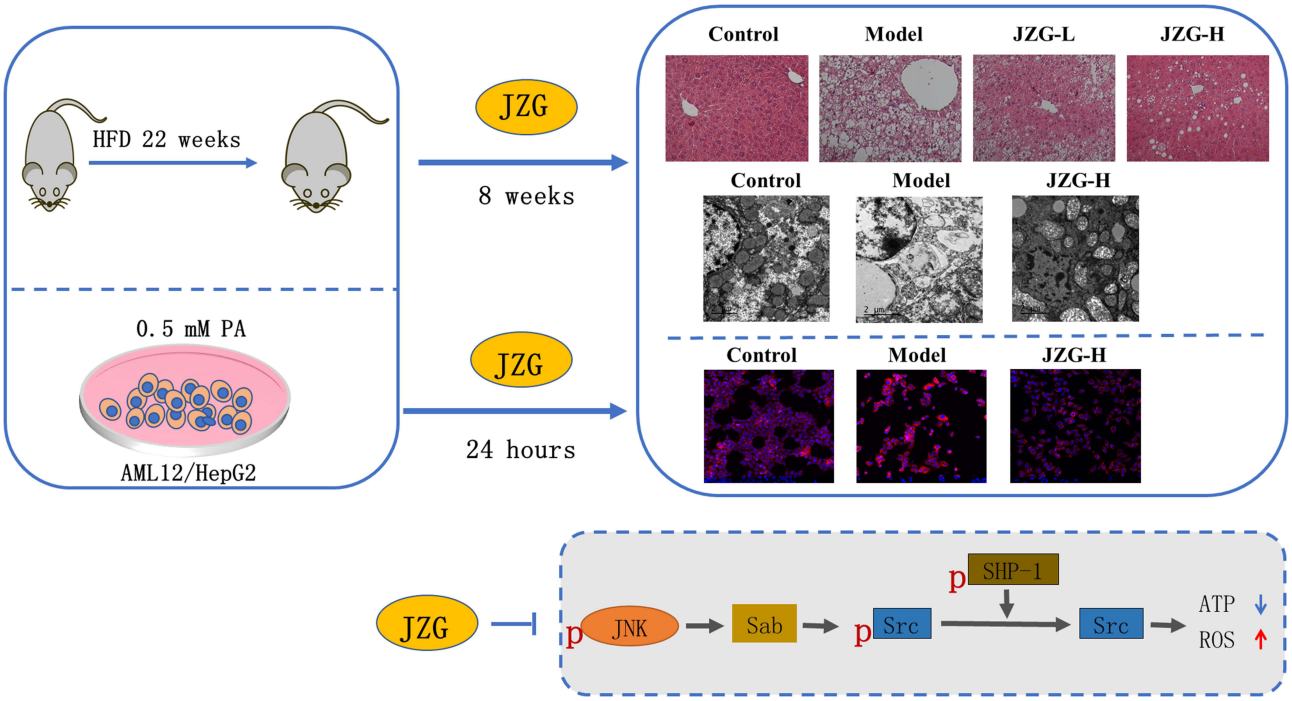

mitochondrial dysfunction, oxidative stress, lipid peroxidation, and endoplasmic reticulum stress, ultimately resulting in hepatocellular injury.[5–7] As mitochondria are key organelles involved in energy metabolism, their role in the development of NASH has garnered increasing attention.[8,9] Mitochondrial dysfunction has been observed in patients with NASH[10] and has been further confirmed by cell and animal models.[11,12] The severity of this dysfunction correlates positively with the progression of NAFLD.[13] Mitochondrial dysfunction not only induces oxidative stress and lipid accumulation but also causes hepatocyte damage, thereby facilitating the transition from NAFL to NASH. Moreover, it is noteworthy that excessive FAs in NASH can activate c-Jun N-terminal kinase (JNK) signaling. This pathway can interact with the mitochondrial membrane, initiating a cascade of protein alterations that ultimately lead to mitochondrial damage.[14]

To date, Resmetirom, an thyroid hormone receptor-β agonist, is the only one specific drug approved for NAFLD treatment. But research is still needed to confirm its clinical efficacy and safety.[15] And the primary treatment approach remains lifestyle modification, which is too strict to persist for many patients.[16] In recent decades, accumulating evidence has highlighted the potential of traditional Chinese medicine (TCM) in the prevention and treatment of NASH.[17] In TCM theory, "spleen deficiency, phlegm, and stasis" is considered the underlying pathogenesis of NAFLD.[18] Based on this theory, our research group developed the TCM formula Jiangzhi Granule (JZG) (alternatively named Salvia–Nelumbinis naturalis), composed of five herbal medicines. In vitro studies have shown that JZG can reduce fatty acid-induced lipid droplet accumulation and hepatocyte damage.[19,20] Several studies have also demonstrated that JZG can improve histopathological changes in liver tissues and serum lipid levels in rodent models of NASH.[19,21,22] However, its mechanism has been incompletely elucidated by far. Our previous research found that JZG could inhibit JNK activation in the liver tissues of NASH mice induced by a methionine-and choline-deficient (MCD) diet.[23] Therefore, in this study, using the in vitro and in vivo NASH models, we aim to explore whether JZG can mitigate lipotoxic liver injury in NASH by improving mitochondrial dysfunction through the regulation of JNK signaling. This could further support the use of JZG as a clinical alternative for NASH treatment.

Materials and Methods

Drugs Preparation

The formula JZG consists of five herbal medicines, with the following daily doses for adult use: *Gynostemma pentaphyllum* (Thunb). Makino 15 g, *Polygonum cuspidatum* Sieb. *et* Zucc 15 g, *Salvia miltiorrhiza* Bunge 9 g, *Nelumbo nucifera* Gaertn 6 g, and *Artemisia capillaris* Thunb 9 g. The raw herbs, supplied by the Pharmacy Department of Longhua Hospital, Shanghai University of TCM, were mixed and extracted with water. After filtration, the extract was further processed with ethanol, and the final extract powder was obtained through lyophilization. The chemical constituents of the formula had been analyzed using UPLC-TOF-MS.[24]

Cell Culture and Treatment

Hepatocyte cell lines AML12 and HepG2 were obtained from the Institute of Cell Biology, Chinese Academy of Science (Shanghai, China). Cells were cultured in DMEM supplemented with 10% FBS and 1% penicillin/streptomycin (Gibco, Lonsera, Grand Island, United States) at 37 °C in a 5% CO_2 atmosphere. The cells incubated in DMEM with palmitic acid (PA), 1% BSA and, and 5% FBS (Sigma, Steinheim, Germany) or in DMEM only with 1% BSA and 5% FBS for 24 h were used as the model group or control group separately. For the JZG treatment group, cells were co-incubated with PA and JZG dissolved in DMEM at different doses.

Cell Viability Test

AML12 and HepG2 cells were cultured in 96-well plates with 5×10^3 cells per well. To select the dose to trigger lipotoxic injury in vitro, cells were incubated with PA at different dose (0.1, 0.25, 0.5, 1, 1.5, 2 mm) for 24 h. Subsequently, the CCK-8 reagent (Dojindo, Kumamoto, Japan) was added at a 1:10 ratio with DMEM, and incubated at 37 °C for 4 h. Optical density (OD) at 450 nm was measured using a microplate reader (BioTeck, Winooski, United States). Cell viability was calculated using the formula: $\text{Cell viability}(\%) = \frac{\text{OD450 [treated]} - \text{OD450 [blank]}}{\text{OD450 [control]} - \text{OD450 [blank]}} \times 100\%$. Additionally, cell viability test was also performed for the hepatocytes after 24 h-incubation with JZG (0.125, 0.25, 0.5, 1, 2, 4, 8, 16 μg/mL) to primarily determine the safe dose of the drug. Further, PA (0.5 mm) and varying concentrations of JZG were added to the cells, followed by a 24-hour incubation and the viability was measured by CCK8 assay.

Nile Red Staining of Cells

After fixation with 4% paraformaldehyde for 30 min, the cells were stained with Nile red solution (SIGMA, Steinheim, Germany) for 20 min, followed by DAPI staining (MP, Biomedicals, United States) for 10 min. Images were captured and fluorescence values were analyzed using ImageXpress microsystem High Content Imaging System (Molecular Devices, LLC. San Jose, CA, United US). The ratio of Nile red dots per cell was determined as: Nile red dots/cells = Cell integrated intensity/Total number of cells.

TMRM Fluorescence Staining and ATP Determination

Cells were incubated with tetramethyl rhodamine, methyl ester (TMRM) staining solution (Sigma) for 20 min. Fluorescence images were acquired using the ImageXpress Microsystem High-content imaging system. To detect ATP generation in cells, cells were lyzed and mixed with an ATP detection working solution (Beyotime, Hangzhou, China). The relative luminescence units (RLU) were measured by the microplate reader, and ATP content was calculated based on a standard curve.

Design of Mice Experiment

Six-week-old male C57BL/6J mice were obtained from Shanghai Slack Laboratory Animal Co. Ltd. The mice were housed at a temperature of 22±2 °C and a humidity range of 50–70%. The experimental protocols were approved by the Animal Experiment Ethics Committee of Shanghai University of Traditional Chinese Medicine, with the Ethics Permission Number LHERAW-23031. All the procedures were carried out in accordance to the guide for the care and use of laboratory animals (National Research Council (US) Committee for the Update of the Guide for the Care and Use

of Laboratory Animals. 8th ed). The mice were randomly assigned to four groups based on their body weights (8 mice per group): Control group, fed a standard diet; HFD group, fed a high-fat diet (HFD, the calorie percentages from fat, carbohydrate, and protein are 20%, 20%, and 60%, respectively, Research diet, Cat:D12492, New Brunswick, USA) for 30 weeks; JZG-L group and JZG-H group, fed a HFD and gavaged with JZG daily at 7.7 mg/kg and 14.14 mg/kg, respectively for the last 8 weeks of the study. The dosage was determined based on clinical dose conversion relative to mouse weight. At the end of the study, the mice were euthanized, and blood and liver tissue samples were collected for further experimental analysis.

Liver Histopathology and Immunohistochemistry

Liver samples were fixed in 4% neutral formalin for 24 hours, then dehydrated and embedded in paraffin. Subsequently, The samples were sectioned into 4 μm slices, deparaffinized, rehydrated, and stained with hematoxylin and eosin (HE) staining solution (Yixin, Shanghai, China). The slides were mounted and visualized under a light microscope (Nikon ECLIPSE 50i, Tokyo, Japan).

For the immunohistochemical analysis, the deparaffinized liver sections were first treated with 0.01M citrate buffer at a pH of 6.0 using a high-pressure heating device for 10 minutes to retrieve antigens. The sections were then blocked to prevent non-specific binding, and then incubated overnight at 4 °C with an antibody against 4-hydroxynonenal (4-HNE) (Alpha Diagnostic, Texas, United States). An Envision+ secondary antibody from Dako (Glostrup, Denmark) was applied for 1 hour at room temperature. Then the chromogen substrate (DAB) was used to develop a brown coloration at the sites of positive staining, followed by counterstaining with hematoxylin.

Transmission Electron Microscopy of Liver Tissues

To examine the mitochondrial structure, liver samples were immersed in 2% glutaraldehyde for a duration of 2 h, then further sectioned into ultra-thin slices with a thickness of 70 nm. Detailed subcellular images were captured using a transmission electron microscope (HITACHI H-7650).

Quantitative RT-PCR

Total RNA was extracted from liver tissues and cells using Trizol reagent (Invitrogen, USA). The RNA was then reverse transcribed into complementary DNA (cDNA) using a reverse transcription kit (Applied Biosystems, Carlsbad, CA, United States). The quantitative polymerase chain reaction (RT-PCR) was performed using a SYBR Green PCR Mix kit (Accurate Biology, Changsha, China) on StepOnePlus Real-Time PCR System (Applied Biosystems). The PCR primers were synthesized by Shanghai Shinegene Bio-tech Co., Ltd. The sequences were listed in Table 1. Relative mRNA levels were calculated using the $2^{-\Delta\Delta Ct}$ calculation method, with the housekeeping gene β-actin serving as the internal reference gene for normalization.

Table 1 The PCR Primer Sequences Utilized in the Study

Gene	Sequence (5'-3')
m β-actin	Forward: GAGACCTTCAACACCCCAGC
	Reverse: ATGTCACGCACGATTTCCC
m PGC-1α	Forward: TGGCACGCAGCCCTATTC
	Reverse: GAGGATCTACTGCCTGGGGAC
m NRF1	Forward: TCCCAGAGATGCTCAAGTATTCC
	Reverse: TTAACTATGGTCCGTAATGCCTG
m TFAM	Forward: GCATCCCCTCGTCTATCAGTC
	Reverse: TGTGGAAAATCGAAGGTATGAAC

Western Blot

The BCA method was employed to quantify protein concentrations from cell or liver tissue lysates prepared using RIPA buffer. The proteins were resolved via acrylamide gel electrophoresis and subsequently transferred onto a PVDF membrane (Millipore, Billerica, USA). Following blocking, the membrane was incubated with a range of primary antibodies, including those against phospho-JNK (P-JNK), total JNK (JNK), total non-receptor tyrosine kinase c-Src (Src), phospho-Src (P-Src), total SH2-containing protein tyrosine phosphatase (SHP-1), phospho-SHP-1 (P-SHP-1), PGC-1, Sab, Cleaved PARP, and β-actin (Cleaved PARP from ABclonal, Wuhan, China; Sab from Proteintech, Wuhan, China; all other antibodies from Cell Signaling, Massachusetts, United States). These primary antibodies were applied and incubated with the membrane at 4 °C overnight. The next day, the membrane was further incubated with appropriate secondary antibodies, followed by exposure to ECL solution (Millipore). The protein bands were visualized using a chemiluminescence imaging system (Tanon, Shanghai, China).

Statistical Analysis

The data were presented as the mean ± standard deviation (SD). To compare the means of two distinct groups, a Student's *t*-test was employed. For comparisons among three or more groups, a one-way analysis of variance (ANOVA) was utilized. Data analysis and graphical representations were carried out using SPSS 28.0 software from SPSS Inc. (Chicago, Illinois) and GraphPad Prism 9.0 from GraphPad Software Inc. (San Diego CA, United States). And $p < 0.05$ was considered statistically different.

Results

JZG Mitigated Lipotoxic Injury of Hepatocytes

As illustrated in Figure 1A, the cell viability of HepG2 and AML12 cells was reduced by PA in a dose-dependent manner. The cell survival rate was approximately 50% when induced by 0.5 mm PA, which was selected for subsequent experiments. After incubation with various concentrations of JZG, ranging from 0.125 to 16 μg/mL cells for 24h, a significant reduction in cell viability was only observed when the JZG concentration reached 8 μg/mL and more. Furthermore, Figure 1B demonstrated that the viability of HepG2 and AML12 cells was reduced upon exposure to 0.5 mm PA, which was alleviated by JZG at a concentration of 0.5 μg/mL. This does of JZG was thereby subsequently chosen for further in vitro studies.

Nile red staining was used to show the neutral lipid droplets in the hepatocytes. The acquired images and the calculated fluorescence intensity/cell results demonstrated that JZG treatment markedly attenuated lipid accumulation caused by PA incubation (Figure 1C). Moreover, as illustrated in Figure 1D, Western blot analysis revealed that JZG significantly decreased the levels of cleaved PARP, a protein marker of apoptotic process.

JZG Improved PA-Induced Mitochondrial Dysfunction in Hepatocytes

Mitochondrial function was assessed using TMRM staining to evaluate changes in mitochondrial membrane potential. As shown in Figure 2A, PA caused a significant reduction in TMRM fluorescence intensity in both HepG2 and AML12 cells, indicating occurrence of mitochondrial dysfunction. This impairment was notably reversed by incubation with JZG. Furthermore, JZG also restored PA-induced reductions in ATP generation in hepatocytes (Figure 2B). PGC-1α plays a crucial role in mitochondrial biogenesis and oxidative phosphorylation, leading to increased mitochondrial number and activity. As depicted in Figure 2C, JZG intervention significantly prevented the down-regulation of PGC-1α protein expression induced by PA.

JZG Inhibited PA-Induced Activation of the JNK Signaling Pathway in Hepatocytes

This study assessed the protein levels of key components in the JNK signaling pathway, including JNK, phospho-JNK (P-JNK), Sab, SH2-containing protein tyrosine phosphatase (SHP-1), phospho-SHP-1 (P-SHP-1), non-receptor tyrosine kinase c-Src (Src), phospho-Src (P-Src), as well as the ratios of P-JNK/JNK, P-SHP-1/SHP-1 and P-Src/Src in HepG2 and AML12 cells. In contrast to the control group, the ratios of P-JNK/JNK and P-SHP-1/SHP-1 were significantly

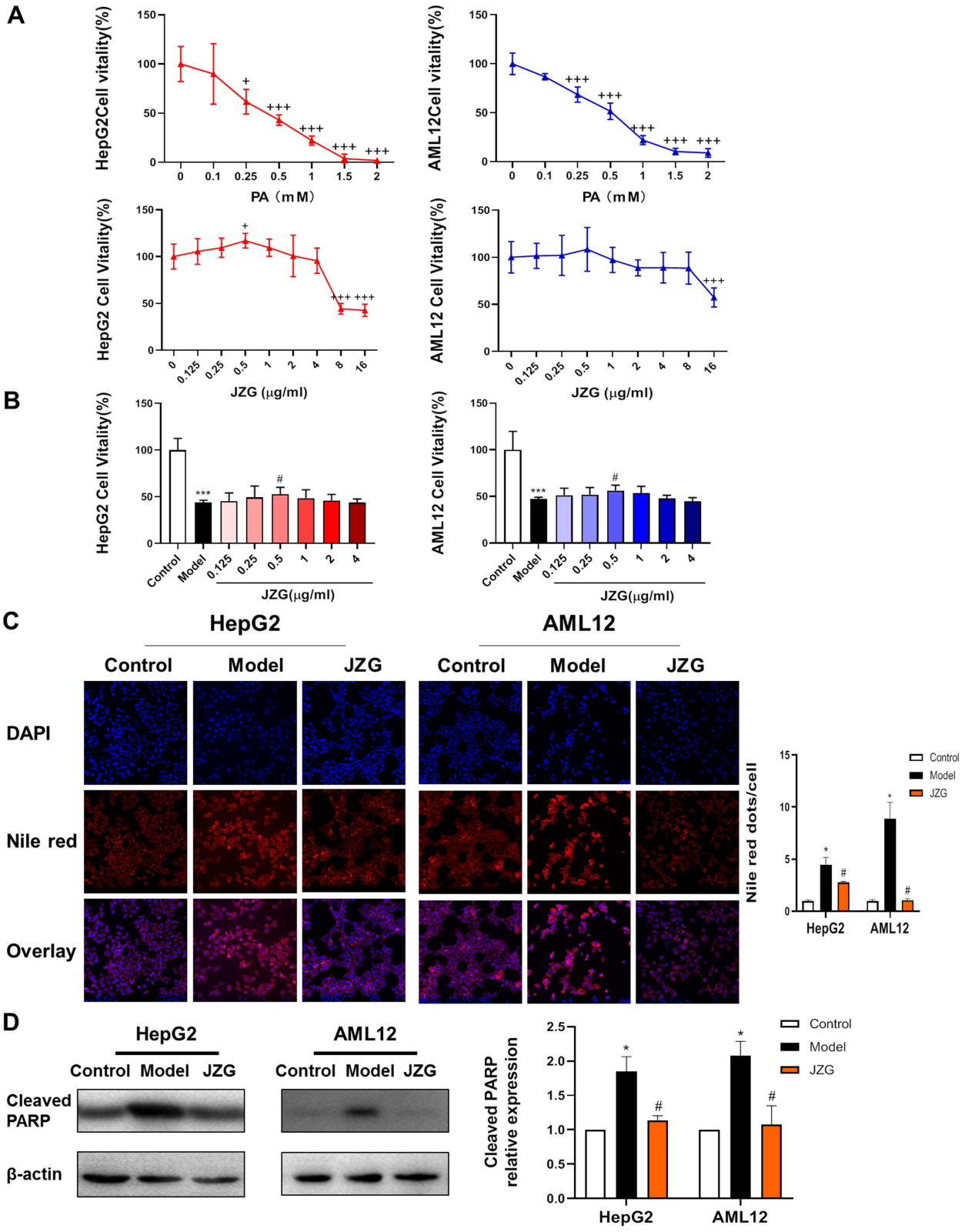

Figure 1 JZG ameliorated lipotoxic damage in hepatocytes induced by PA. (**A**) Effect of JZG on hepatocyte viability in normal culture medium. (**B**) Impact of JZG on hepatocyte viability under PA-induced conditions. (**C**) DAPI and Nile Red double staining of hepatocytes subjected to lipotoxic injury (200× magnification). (**D**) Effect of JZG on the level of Cleaved PARP in PA-induced hepatocytes. $^{+}p < 0.05$, $^{+++}p < 0.001$ vs JZG (0); $^{*}p < 0.05$, $^{***}p < 0.001$ vs Control; $^{\#}p < 0.05$ vs Model.

https://doi.org/10.2147/DMSO.S492174

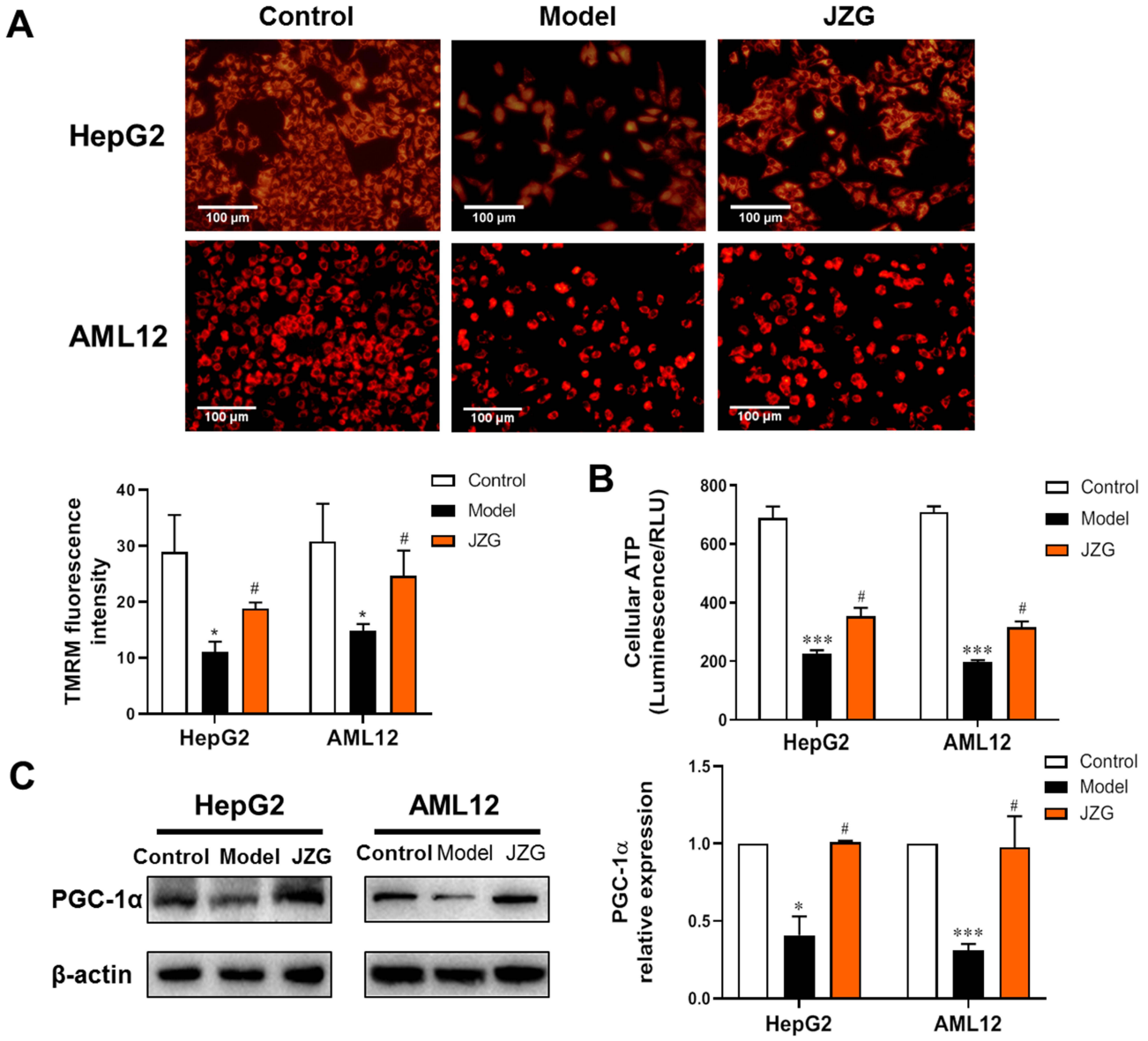

Figure 2 JZG alleviated mitochondrial impairment in hepatocytes induced by PA. (**A**) TMRM staining of hepatocytes (200× magnification). (**B**) Quantification of cellular ATP synthesis in hepatocytes. (**C**) Protein expression levels of PGC-1α in hepatocytes. *$p < 0.05$, ***$p < 0.001$ vs Control; $^{\#}p < 0.05$ vs Model.

elevated, while the ratio of P-Src/Src was markedly reduced in the model cells induced by PA. In comparison to the model group, JZG treatment led to a decrease in the ratios of P-JNK/JNK and P-SHP-1/SHP-1, with a notable increase in the ratio of P-Src/Src (Figure 3).

JZG Alleviated Lipotoxic Liver Injury in NASH Mice

Dietary-based rodent NAFLD models are considered the most suitable models. HFD-fed male C57BL/6J mice are most frequently utilized, which closely resemble human NAFLD with insulin resistance and metabolic syndrome. Longer period intake of HFD could induce the histological changes of NASH in mouse liver, including steatosis, hepatocyte ballooning, lobular inflammation, and perisinusoidal fibrosis.[25] Figure 4A–C showed that, after being fed HFD for 30 weeks, the model mice exhibited a significant increase in body weight, liver weight, and levels of serum total cholesterol (TC), HDL cholesterol (HDL-c), LDL cholesterol (LDL-c), alanine aminotransferase (ALT), aspartate aminotransferase (AST), and lactate dehydrogenase (LDH). Compared to the HFD group, mice treated with both low and high doses of JZG showed significant

https://doi.org/10.2147/DMSO.S492174

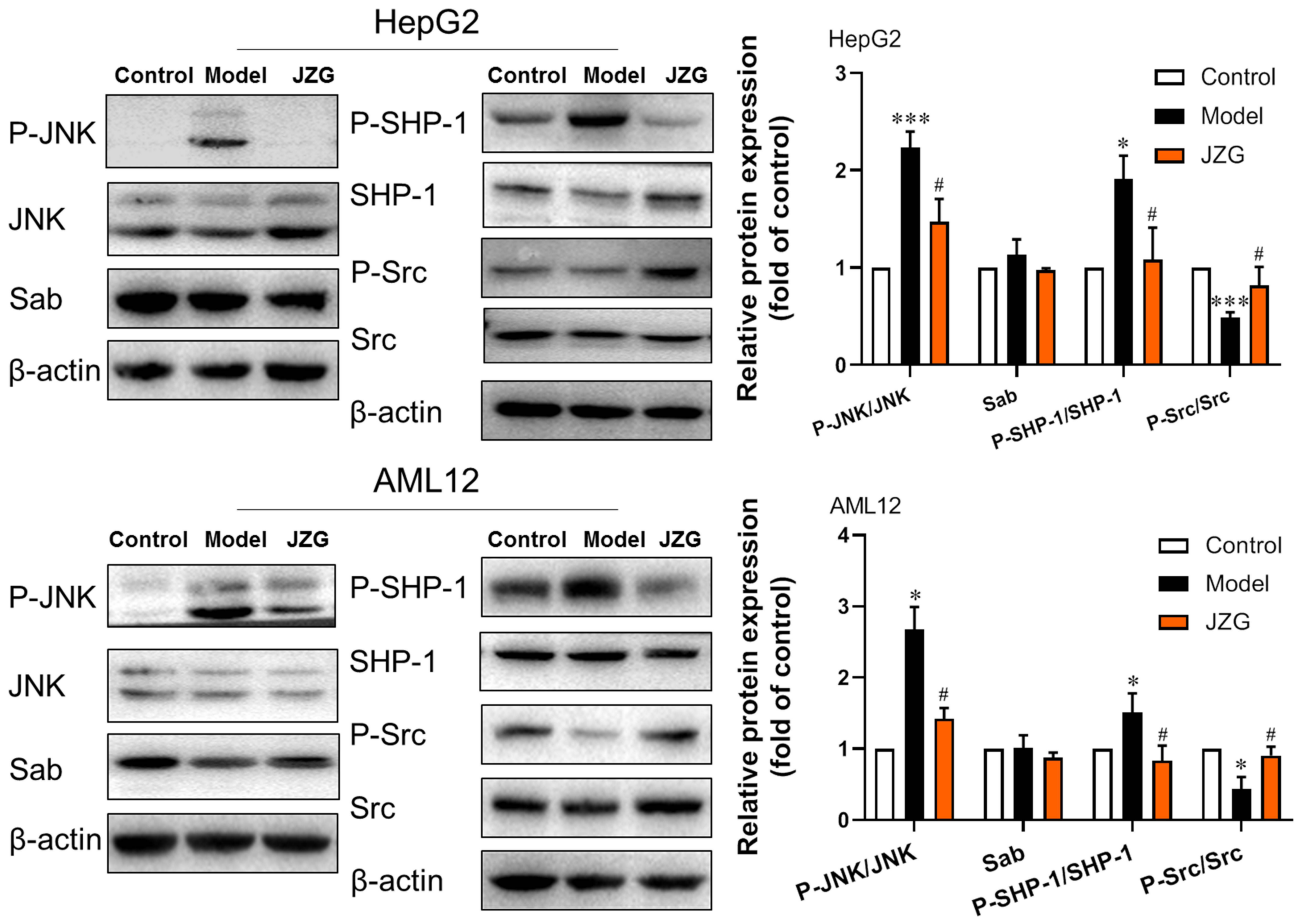

Figure 3 JZG suppressed the activation of the JNK signaling in hepatocytes induced by lipotoxicity. The expression/activation levels of JNK, SHP-1, Src, and Sab proteins in hepatocytes were detected using Western blot analysis. $^{*}p < 0.05$, $^{***}p < 0.001$ vs Control; $^{\#}p < 0.05$ vs Model.

reductions in these parameters. Histopathological analysis using HE staining revealed extensive lipid accumulation, hepatocyte ballooning degeneration, and inflammatory cell infiltration in the liver tissues of HFD mice, confirming the establishment of the NASH model (Figure 4D). Treatment with JZG notably improved these liver histopathological features (Figure 4D). Additionally, cleaved PARP, which was significantly upregulated in the liver tissues of model mice compared to controls, was effectively reduced by JZG intervention (Figure 4E).

JZG Mitigated JNK Signaling Activation and Improved Mitochondrial Function in the Liver Tissues of NASH Mice

The transmission electron microscopy images of liver tissues demonstrated that HFD resulted in a significant reduction in mitochondrial quantity, with mitochondria exhibiting enlarged and damaged morphology in hepatocytes (Figure 5A). With JZG intervention, there was an observed increase in mitochondrial number and a partial restoration of their typical structure. Compared with model group, there were less and smaller lipid droplets in the JZG group. In liver tissues of model mice, the expression levels of genes associated with mitochondrial biogenesis and function, including PGC-1α, NRF1, and TFAM, were found to be diminished, which were upregulated by JZG treatment, as depicted in Figure 5B. This indicates the protective effects for mitochondrial function of the TCM formulation.

Mitochondrial dysfunction is known to generate excessive reactive oxygen species (ROS), which can trigger lipid peroxidation and subsequent cellular damage. Elevated levels of 4-hydroxynonenal (4-HNE), a marker of lipid peroxidation, were detected in the liver tissues of model mice compared to control mice. JZG treatment significantly reduced the intensity of 4-HNE staining (Figure 5C). Additionally, the expression levels of JNK pathway-related molecules in

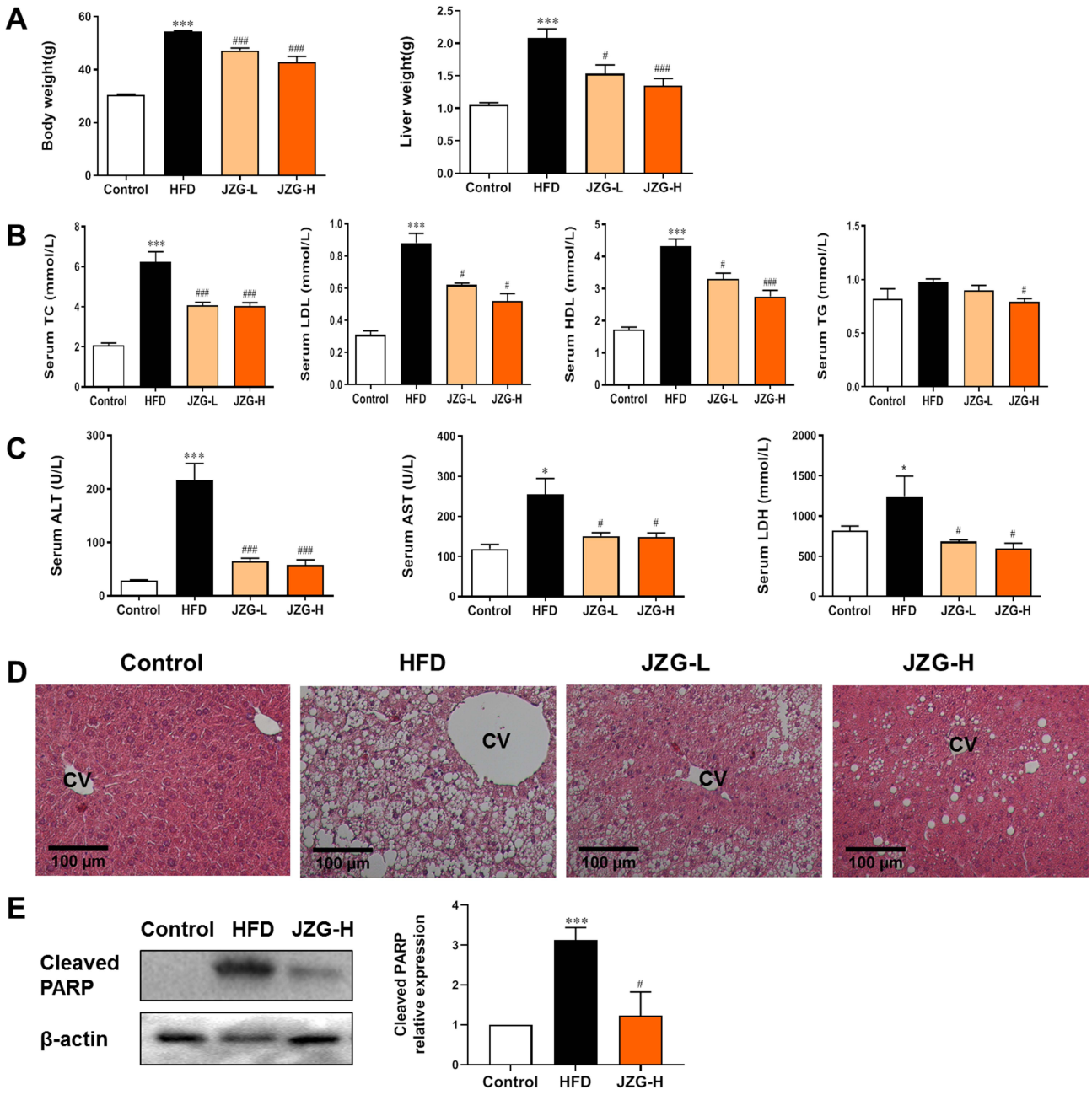

Figure 4 The effect of JZG on NASH mice. (**A**) Changes in body and liver weights of the mice. (**B**) Serum lipid levels. (**C**) Serum levels of ALT, AST and LDH. **(D)** HE staining of liver tissues, with the central vein (CV) indicated (200× magnification). (**E**) Expression of cleaved PARP protein in mice liver tissues. $^{*}p < 0.05$, $^{***}p < 0.001$ vs Control; $^{\#}p < 0.05$, $^{\#\#\#}p < 0.001$ vs HFD group.

mice liver tissues were shown in Figure 5D. There was no difference in Sab expression among different group. High dose of JZG notably decreased the ratios of P-JNK/JNK and P-SHP-1/SHP-1, while increasing the P-Src/Src ratio in the liver tissues of NASH mice. This suggests that JZG effectively inhibits the activation of the JNK signaling pathway.

Discussion

Compared with NAFL, NASH increases the risk of developing poor outcomes, including liver cirrhosis, liver failure, hepatocellular cancer, cardiovascular disease, and malignancy.[26,27] Thus early prevention and reversal of NASH development are crucial. Currently, some drugs in Phase 2 and 3 clinical trials target mainly metabolic pathways (the PPAR agonist pioglitazone,[28] the FXR agonist Obecchic acid[29]), cellular stress and apoptosis,[30] and the immune pathway[31] and

https://doi.org/10.2147/DMSO.S492174

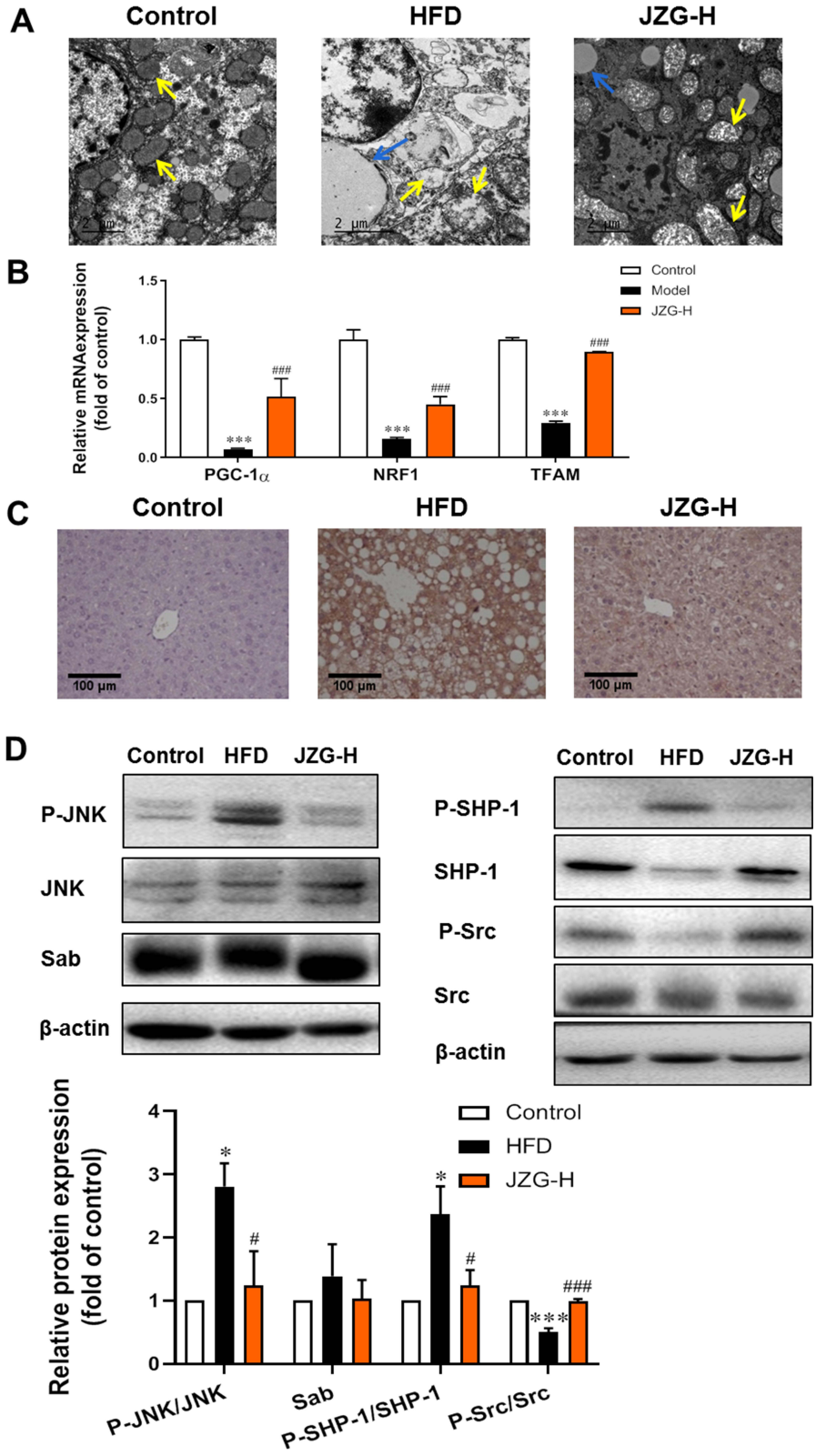

Figure 5 The impact of JZG on mitochondrial function and the JNK signaling pathway in the liver tissues of NASH mice. (**A**) Electron microscopy images of liver tissues (yellow arrow: mitochondria; blue arrow: lipid droplets) (20000× magnification). (**B**) mRNA levels of PGC-1α, NRF1, and TFAM in liver tissues of mice. (**C**) IHC staining of 4-HNE in liver tissues (200×). (**D**) Expression/activation levels of JNK pathway-related molecules. *$p < 0.05$, ***$p < 0.001$ vs Control; $^{\#}p < 0.05$, $^{\#\#\#}p < 0.001$ vs HFD group.

https://doi.org/10.2147/DMSO.S492174

so on. The efficacy and safety of these new emerging drugs need to be further investigated. By far, there is only one specific drug approved for NAFLD treatment,[32] highlighting the need for the development and application of new drugs.

Recent pharmacological studies have exhibited the benefits and effects of TCM in treating NAFLD/NASH.[33,34] The TCM herbal formula JZG has been used clinically for NAFLD treatment. A multicenter clinical trial showed that JZG effectively reduced the body mass index (BMI), ALT, and serum lipid levels in NAFL patients without adverse reactions.[35] Previous in vivo researches indicated that JZG improved the HFD-induced hepatosteatosis and metabolic abnormalities in NAFLD mice,[20,22] and ameliorated the histological assessment of NAFLD activity score of MCD diet-induced NASH mice.[23] In this study, 8-week treatment with JZG significantly decreased body and liver weight, serum lipid and liver enzyme levels, and apoptosis-related molecule in liver tissues of the HFD-induced NASH mice. Especially the degree of hepatosteatosis, inflammatory infiltration, and ballooning degeneration in the liver tissues of model mice were ameliorated by JZG. Additionally, in vivo experiments showed that Lipid droplet accumulation in PA-treated hepatocytes could be significantly attenuated by JZG.[19] This study found JZG not only reduced lipid deposition, but also improved cell apoptosis and increased cell viability.These results confirmed JZG's beneficial effects on the lipotoxic liver injury in NASH. Previous clinical study has shown that routine dose of JZG can improve hepatosteatosis and blood lipid levels in NAFL patients.[35] In this study, JZG was applied at both a low dose equivalent to the clinical routine dose, and a high dose, which is twice the low dose. The results showed that JZG-H have better effects on mouse liver histopathology, body weight, liver weight and blood lipids than JZG-L. This suggests that the use of higher dose of JZG may be considered to achieve better therapeutic effect in future clinical NASH studies.

Studies have evidenced the decline in hepatic mitochondrial functionality, such as decreased ATP repletion and ETC complex activity. Hepatic mitochondrial oxidative capacity was proven in human biopsy-proven NASH. The ultrastructural cell image displays mitochondrial defects like loss of mitochondrial cristae, paracrystalline inclusions in swollen mitochondria.[10] There are defects in mitochondrial biogenesis, with its biomarkers such as PGC-1α, NRF1, TFAM and SIRT1 significantly diminish in NASH mouse models.[11] Abnormal mitochondrial function, leading to impaired fatty acid oxidation and oxidative phosphorylation, drives oxidative stress, which is an important feature of human NASH. The excessive accumulation of ROS can damage mt-DNA directly and participate in lipid peroxidation reactions to cause cell injury.[10] In our study, abnormal changes in the number and morphology of mitochondria, and the expression of mitochondrial synthesis or activity-related molecules including PGC-1α, NRF1, and TFAM in NASH mice were reverted by JZG treatment. Lipid peroxide HNE was also observed decreased in JZG group compared with model group. Additionally, in vitro results showed lowerTMRM intensity and ATP generation in PA-induced hepatocytes, which were upregulated by JZG. These results support the ameliorating effect of JZG for mitochondrial dysfunction and lipotoxic damage in hepatocytes.

By applying UPLC-TOF-MS technology combined with network pharmacology analysis, 50 potential target molecules of JZG for NASH treatment were predicted, including mitogen-activated protein kinase (MAPK).[24] The MAPK signaling pathways activated by various external stressors such as nutrients, extracellular matrix, and drugs, play a crucial role in liver injury-related diseases, including drug-induced hepatotoxicity, viral hepatitis, NAFLD/NASH, liver fibrosis, and cancer.[14,36,37] MAPK includes three major signaling pathways: extracellular signal-regulated kinase (ERK), the p38 kinase, and the JNK, with JNK acting as a primary effector in regulating liver injury. JNK activation is generally transient and can be inhibited by subsequently activated NF-κB signaling, while persistent JNK activation status is positively correlated with liver damage.[36,38] It has been reported that free fatty acids were able to induce sustained JNK activation, with PA causing more pronounced hepatocellular toxicity.[39] Additionally, cell damage and apoptosis could be ameliorated by JNK inhibitors by blocking the sustained JNK-Bim-mediated Bax activation. In this study, the higher ratio of Phospho-JNK/JNK expression was also observed in both the PA-induced hepatocytes and liver tissues of NASH mice, and JZG treatment attenuated aberrant JNK activation. This is consistent with our previous in vivo study, JZG intervention prevented the upregulation of phosphorylated JNK in liver tissues of NASH mice induced by MCD diet.[23]

Research by Win S[40] demonstrated that PA could trigger mitochondrial impairment and cell demise in primary mouse hepatocytes via the JNK/Sab-intramitochondrial pathway. Under stress conditions, JNK activation leads to its translocation and specific binding to the mitochondrial protein Sab, causing a conformational change in Sab and detachment of SHP-1. SHP-1, once phosphorylated by Src, deactivates Src through phosphorylation. This sequence disrupts mitochondrial electron transport, increases ROS generation, and ultimately causes mitochondrial dysfunction.[41–43] Our investigation observed

increased SHP-1 activation and decreased Src activation in hepatocytes subjected to PA or in the liver tissues of NASH mice, with these changes significantly reversed by JZG intervention. Therefore, JZG might exert the function on NASH through regulating the JNK/Sab/Src pathway.

Noteworthy, due to containing many various components, TCM has the characteristic of multi-target. Previous studies have found that JZG improved NAFLD or NASH through multiple approaches including regulation of lipid metabolism via SIRT1/AMPK signaling, promotion of PI3K-AKT-mTOR-mediated autophagy,[20,22] inhibition of oxidative stress,[23] endoplasmic reticulum stress[21] or TNF/NFκB inflammatory signaling pathway.[24] This study expands the regulation of JNK-mediated mitochondrial dysfunction as one of its mechanisms. JNK plays a central role in cell stress. Although there are studies found JNK inhibitor was able to protect the mouse liver from HFD-induced hepatosteatosis, inflammation and fibrosis,[44] the role of JNK in the progression of metabolic complications need to be better understood before developing drugs for the treatment. A study has found that JNK1 ablation exacerbated oxidative damage in the skin in a mouse model of obesity.[45] In addition, NASH is a liver disease with complex pathological mechanisms and heterogeneity. Therefore, compared to JNK inhibitors, JZG with multiple regulatory targets may have better efficacy and safety in clinical applications.

Conclusion

In summary, this study demonstrates that JZG treatment could significantly improve mitochondrial dysfunction and reduce lipotoxic liver injury in NASH in vivo and in vitro models. The inhibitory regulation of the JNK/Sab/Src signaling pathway may contribute to one of the underlying mechanisms of JZG in preventing and reversing NASH development. These findings is beneficial to support the clinical use of JZG as a treatment option for NASH. The limitation of the simple HFD-fed model used in this study is unable to reach more advanced stages, such as fibrosis and cirrhosis. Future studies for JZG effect and mechanism would be carried out by using high-fat/high-fructose diets to induce NASH model with more serious liver injury. Furthermore, simultaneous application of JNK agonists in the treatment possibly help increase evidence to clarify JZG's effects on mitochondrial function are JNK-dependent. Additionally, further clinical studies are needed to validate JZG's efficacy and safety.

Data Sharing Statement

The datasets used and /or analyzed during the current study are available from the corresponding author (Haiyan Song) upon reasonable request.

Ethics Approval and Informed Consent

The animal study protocol was approved by the Experimental Animal Care and Use Committee of Shanghai University of Traditional Chinese Medicine (IACUC NO.: LHERAW-23031, 2021).

Funding

This research was funded by National Natural Science Foundation of China (No. 82374417, 82174287 and 82274386), Science and Technology Development Fund of Shanghai University of Traditional Chinese Medicine (No. 23KFL069).

Disclosure

The authors report no conflicts of interest in this work.

References

1. Scorletti E, Carr RM. A new perspective on NAFLD: focusing on lipid droplets. *J Hepatol*. 2022;76(4):934–945. doi:10.1016/j.jhep.2021.11.009
2. Younossi ZM, Golabi P, Paik JM, et al. The global epidemiology of nonalcoholic fatty liver disease (NAFLD) and nonalcoholic steatohepatitis (NASH): a systematic review. *Hepatology*. 2023;77(4):1335–1347. doi:10.1097/HEP.0000000000000004
3. Friedman SL, Neuschwander-Tetri BA, Rinella M, Sanyal AJ. Mechanisms of NAFLD development and therapeutic strategies. *Nat Med*. 2018;24(7):908–922. doi:10.1038/s41591-018-0104-9
4. Adam R, Karam V, Cailliez V. Annual report of the European Liver Transplant Registry (ELTR) - 50-year evolution of liver transplantation. *Transpl Int*. 2018;31(12):1293–1317. doi:10.1111/tri.13358
5. Woods CP, Hazlehurst JM, Tomlinson JW. Glucocorticoids and non-alcoholic fatty liver disease. *J Steroid Biochem Mol Biol*. 2015;154:94–103. doi:10.1016/j.jsbmb.2015.07.020

6. Li X, Wang Y, Wang H, Huang C, Huang Y, Li J. Endoplasmic reticulum stress is the crossroads of autophagy, inflammation, and apoptosis signaling pathways and participates in liver fibrosis. *Inflamm Res*. 2015;64(1):1–7. doi:10.1007/s00011-014-0772-y
7. Takaki A, Kawai D, Yamamoto K. Molecular mechanisms and new treatment strategies for non-alcoholic steatohepatitis (NASH). *Int J Mol Sci*. 2014;15(5):7352–7379. doi:10.3390/ijms15057352
8. Jakob V. Commentary: mitochondria are more than just the cells' powerhouse. *J Thorac Cardiovasc Surg*. 2020;160(2):e33–e34. doi:10.1016/j.jtcvs.2019.07.029
9. Patterson RE, Kalavalapalli S, Williams CM, et al. Lipotoxicity in steatohepatitis occurs despite an increase in tricarboxylic acid cycle activity. *Am J Physiol Endocrinol Metab*. 2016;310(7):E484–E494. doi:10.1152/ajpendo.00492.2015
10. Fromenty B, Roden M. Mitochondrial alterations in fatty liver diseases. *J Hepatol*. 2023;78(2):415–429. doi:10.1016/j.jhep.2022.09.020
11. Zhao Y, Zhou Y, Wang D, et al. Mitochondrial dysfunction in metabolic dysfunction fatty liver disease (MAFLD). *Int J Mol Sci*. 2023;24(24):242417514. doi:10.3390/ijms242417514
12. Wang YC, Kong WZ, Jin QM, Chen J, Dong L. Effects of salvianolic acid B on liver mitochondria of rats with nonalcoholic steatohepatitis. *World J Gastroenterol*. 2015;21(35):10104–10112. doi:10.3748/wjg.v21.i35.10104
13. Morris EM, Rector RS, Thyfault JP, Ibdah JA. Mitochondria and redox signaling in steatohepatitis. *Antioxid Redox Sign*. 2011;15(2):485–504. doi:10.1089/ars.2010.3795
14. Win S, Than TA, Han D, Petrovic LM, Kaplowitz N. c-Jun N-terminal kinase (JNK)-dependent acute liver injury from Acetaminophen or tumor necrosis factor (TNF) requires mitochondrial Sab protein expression in mice. *J Biol Chem*. 2011;286(40):35071–35078. doi:10.1074/jbc.M111.276089
15. Keam SJ. Resmetirom: first Approval[J]. *Drugs*. 2024;84(6):729–735. doi:10.1007/s40265-024-02045-0
16. Younossi ZM, Loomba R, Rinella ME. Current and future therapeutic regimens for nonalcoholic fatty liver disease and nonalcoholic steatohepatitis. *Hepatology*. 2018;68(1):361–371. doi:10.1002/hep.29724
17. Wei-Fan H, Lee-Yan S, Lin HJ, Chang HH. A review of western and traditional Chinese medical approaches to managing nonalcoholic fatty liver disease. *Evid Based Complement Alternat Med*. 2016;2016:6491420. doi:10.1155/2016/6491420
18. Wei HF, Liu T, Xing LJ, Zheng PY, Ji G. Distribution pattern of traditional Chinese medicine syndromes in 793 patients with fatty liver disease. *Zhong Xi Yi Jie He Xue Bao*. 2009;7(5):411–417. doi:10.3736/jcim20090503
19. Zheng Y, Wang M, Zheng P, Tang X, Ji G. Systems pharmacology-based exploration reveals mechanisms of anti-steatotic effects of Jiang Zhi Granule on non-alcoholic fatty liver disease. *Sci Rep*. 2018;8(1):13681. doi:10.1038/s41598-018-31708-8
20. Zheng Y, Wang M, Shu X, Zheng P, Ji G. Autophagy activation by Jiang Zhi Granule protects against metabolic stress-induced hepatocyte injury. *World J Gastroenterol*. 2018;24(9):992–1003. doi:10.3748/wjg.v24.i9.992
21. Yang L, Zhou Y, Song H, Zheng P. Jiang-Zhi granules decrease sensitivity to low-dose CCl4 induced liver injury in NAFLD rats through reducing endoplasmic reticulum stress. *BMC Compl Med Therap*. 2019;19(1):228. doi:10.1186/s12906-019-2641-2
22. Liu Y, Li Y, Wang J, et al. Salvia-Nelumbinis naturalis improves lipid metabolism of NAFLD by regulating the SIRT1/AMPK signaling pathway. *BMC Compl Med Therap*. 2022;22(1):213. doi:10.1186/s12906-022-03697-9
23. Liu Y, Song H, Wang L, et al. Hepatoprotective and antioxidant activities of extracts from Salvia–Nelumbinis naturalis against nonalcoholic steatohepatitis induced by methionine- and choline-deficient diet in mice. *J Transl Med*. 2014;12(1):315. doi:10.1186/s12967-014-0315-x
24. Zhou W, Zhu Z, Xiao X, et al. Jiangzhi Granule attenuates non-alcoholic steatohepatitis by suppressing TNF/NFκB signaling pathway-a study based on network pharmacology. *Biomed Pharmacother*. 2021;143:112181. doi:10.1016/j.biopha.2021.112181
25. Im YR, Hunter H, de Gracia Hahn D. A systematic review of animal models of NAFLD finds high-fat, high-fructose diets most closely resemble human NAFLD. *Hepatology*. 2021;74(4):1884–1901. doi:10.1002/hep.31897
26. Lindenmeyer CC, McCullough AJ. The natural history of nonalcoholic fatty liver disease-an evolving view. *Clin Liver Dis*. 2018;22(1):11–21. doi:10.1016/j.cld.2017.08.003
27. Rinella ME, Sanyal AJ. Management of NAFLD: a stage-based approach. *Nat rev Gastroentero Hepatol*. 2016;13(4):196–205. doi:10.1038/nrgastro.2016.3
28. Ratziu V, Charlotte F, Bernhardt C, et al. Long-term efficacy of rosiglitazone in nonalcoholic steatohepatitis: results of the fatty liver improvement by rosiglitazone therapy (FLIRT 2) extension trial. *Hepatology*. 2010;51(2):445–453. doi:10.1002/hep.23270
29. Mudaliar S, Henry RR, Sanyal AJ, et al. Efficacy and safety of the farnesoid X receptor agonist obeticholic acid in patients with type 2 diabetes and nonalcoholic fatty liver disease - ScienceDirect. *Gastroenterology*. 2013;145(3):574–582. doi:10.1053/j.gastro.2013.05.042
30. Barreyro FJ, Holod S, Finocchietto PV, et al. The pan-caspase inhibitor Emricasan (IDN-6556) decreases liver injury and fibrosis in a murine model of non-alcoholic steatohepatitis. *Liver Int*. 2015;35(3):953–966. doi:10.1111/liv.12570
31. Friedman SL, Ratziu V, Harrison SA. A randomized, placebo-controlled trial of cenicriviroc for treatment of nonalcoholic steatohepatitis with fibrosis. *Hepatology*. 2018;67(5):1754–1767. doi:10.1002/hep.29477
32. Chen VL, Morgan TR, Rotman Y, et al. Resmetirom therapy for metabolic dysfunction-associated steatotic liver disease: October 2024 updates to AASLD practice guidance. *Hepatology*. 2024; 81(1):312–20.
33. Shi KQ, Fan YC, Liu WY, Li L, Chen Y-P, Zheng M-H. Traditional Chinese medicines benefit to nonalcoholic fatty liver disease: a systematic review and meta-analysis. *Mol Biol Rep*. 2012;39(10):9715–9722. doi:10.1007/s11033-012-1836-0
34. Shi T, Wu L, Ma W, Ju L, Shi J. Nonalcoholic fatty liver disease: pathogenesis and treatment in traditional Chinese medicine and western medicine. *Evid Based Complement Alternat Med*. 2020;2020:8749564. doi:10.1155/2020/8749564
35. Pan J, Wang M, Song H, Wang L, Ji G. The efficacy and safety of traditional Chinese medicine (Jiang Zhi Granule) for nonalcoholic fatty liver: a multicenter, randomized, placebo-controlled study. *Evid Based Complement Alternat Med*. 2013;2013:965723. doi:10.1155/2013/965723
36. Seki E, Brenner DA, Karin M. A liver full of JNK: signaling in regulation of cell function and disease pathogenesis, and clinical approaches. *Gastroenterology*. 2012;143(2):307–320. doi:10.1053/j.gastro.2012.06.004
37. Weston CR, Davis RJ. The JNK signal transduction pathway. *Curr Opin Cell Biol*. 2007;19(2):142–149. doi:10.1016/j.ceb.2007.02.001
38. Win S, Than TA, Zhang J, Oo C, Min R, Kaplowitz N. New insights into the role and mechanism of c-Jun-N-terminal kinase signaling in the pathobiology of liver diseases. *Hepatology*. 2018;67(5):2013–2024. doi:10.1002/hep.29689
39. Malhi H, Bronk SF, Werneburg NW, Gores GJ. Free fatty acids induce JNK-dependent hepatocyte lipoapoptosis. *J Biol Chem*. 2006;281(17):12093–12101. doi:10.1074/jbc.M510660200

40. Win S, Than TA, Le BH, García-Ruiz C, Fernandez-Checa JC, Kaplowitz N. Sab (Sh3bp5) dependence of JNK mediated inhibition of mitochondrial respiration in palmitic acid induced hepatocyte lipotoxicity. *J Hepatol*. 2015;62(6):1367–1374. doi:10.1016/j.jhep.2015.01.032
41. Win S, Than TA, Min RWM, Aghajan M, Kaplowitz N. c-Jun N-terminal kinase mediates mouse liver injury through a novel Sab (SH3BP5)-dependent pathway leading to inactivation of intramitochondrial Src. *Hepatology*. 2016;63(6):1987–2003. doi:10.1002/hep.28486
42. Wiltshire C, Matsushita M, Tsukada S, Gillespie D, May G. A new c-Jun N-terminal kinase (JNK)-interacting protein, Sab (SH3BP5), associates with mitochondria. *Biochem J*. 2002;367(Pt 3):577–585. doi:10.1042/bj20020553
43. Liu Q, Rehman H, Krishnasamy Y, Schnellmann RG, Lemasters JJ, Zhong Z. Improvement of liver injury and survival by JNK2 and iNOS deficiency in liver transplants from cardiac death mice. *J Hepatol*. 2015;63(1):68–74. doi:10.1016/j.jhep.2015.02.017
44. Solinas G, Becattini B. JNK at the crossroad of obesity, insulin resistance, and cell stress response. *Mol Metab*. 2016;6(2):174–184. doi:10.1016/j.molmet.2016.12.001
45. Jin L, Wang M, Yang B, et al. A small-molecule JNK inhibitor JM-2 attenuates high-fat diet-induced non-alcoholic fatty liver disease in mice. *Int Immunopharmacol*. 2023;115:109587. doi:10.1016/j.intimp.2022.109587